# Color Formation in Virtual Reality 3D 360º Cameras

***Bartek Pawlik, Veli-Tapani Peltoketo, Ossi Pirinen, and Petri Nenonen***
***Nokia Technologies, Finland***

## Abstract

*In digital camera applications observed color is formed by light reflecting from or transmitted through a medium, observed by a sensor. The final digital value output by a camera is a composite of the spectrum of emitted light, reflectance (or transmittance) properties of a material and spectral response of the observing sensor. In this paper, we demonstrate how even small changes in any of the mentioned properties can cause clearly visible and sometimes unwanted changes in the digital numbers produced by a camera. Additionally, we explore this problem from the point-of-view of a 3D 360º camera, show how these problems are even more severe in this particular case as well as propose a solution relying on accurate measurement of both light as well as camera's response to it.*

## Introduction

While RGB format of the image is widely known and used in most image processing and computer vision applications, the images are formed from a more complex description of the scene in the spectral domain. In particular, color images are formed by the integration of the illuminant spectrum, spectral camera sensitivity and spectral reflectance of the scene [1].

Camera spectral sensitivities are usually measured using a monochromator and a spectrometer [2], with a time-consuming scanning over the wavelength range which tends to be visible spectrum (380 nm – 700 nm). Due to unavoidable variations in the manufacturing process, even sensors of the same type have slightly varying spectral responses [3] which in fact require accurate response measurements done per each camera sensor of interest.

Practical camera spectral responses are never a linear combination of the CIE (International Commission on Illumination) color matching functions [6] and therefore all such sensors fail the Luther condition [10]. As a result, some of the colors will be reproduced better than others when using a simple 3x3 linear color transformation [4], inducing certain colorimetric error. The goal of sensor color calibration is to minimize that error.

In order to spectrally calibrate the camera, in addition to its spectral sensitivity, one needs to know the spectral reflectance (or transmittance) of a set of targets and the spectral power distribution of an illuminant under which the camera calibration is intended to be performed. Whereas the former depends on physical properties of the target and can be known a priori, the latter depends on the illumination under which target is exposed. It's not uncommon to use a set of standard illuminants for that task. We argue that the accuracy of each of these components is of utmost importance in order to reliably reflect the colors of the scene.

A color constancy problem is especially valid in case of 360º cameras where images from multiple sensors are combined together into single panoramic view. Importance of an exact color match escalates even further having a 3D camera able to record separate monoscopic images for left and right eye of the same overlapping scene, which one can later display as a stereo image in for example a virtual reality headset. Even the slightest discrepancy can ruin an overall impression in terms of user experience. Ensuring that each of the sensors produce accurate colors is the first step to obtain desired outcome of the imaging system.

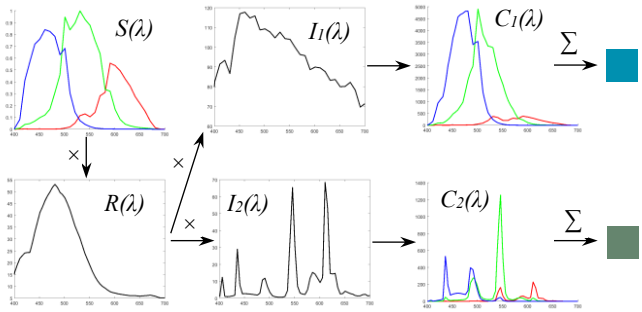


***Figure 1**. Camera measurements under different illuminants. Surface reflectance (R) gets shaped by the spectrum (I) of the scene illuminant which is observed by the camera with spectral sensitivity S. Different illuminants can lead to significantly different trichromatic measurements (C).*

## Preliminaries

Color of a surface that a camera sees ($C_i$, where $i = R,G,B$) under a specific illuminant is a result of an integration of an illuminant spectrum $I(\lambda)$, a surface reflectance spectrum $R(\lambda)$ and camera spectral sensitivity ($S_i(\lambda)$, where $i = R,G,B$):

$$C_i = \int S_i(\lambda)R(\lambda)I(\lambda)d\lambda \qquad (1)$$

Figure 1 depicts the above-mentioned equation in the graphical manner for two different illuminants. The same formula can be used for calculating how the standard observer sees the color, by replacing the camera spectral sensitivities with the standard observer sensitivities and transforming the standard observer seen color values to the target color space, e.g. onto sRGB color space.

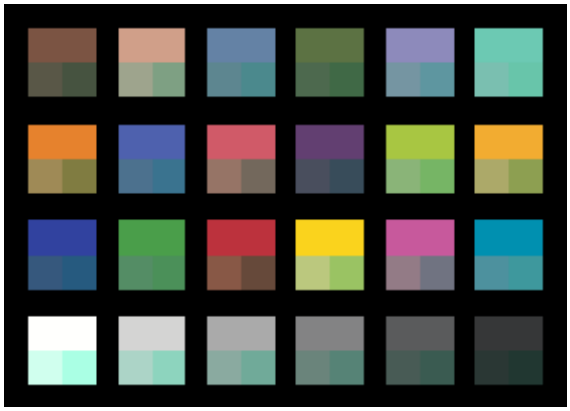

***Figure 2**. Simulated colors of the ColorChecker chart under the standard illuminant D65 seen by two cameras (bottom row at each patch) and reference standard observer simulation based sRGB colors (top row at each patch).*

Camera spectral sensitivities of different camera models might differ from each other significantly. In addition, there is a difference between camera modules of the same type and model. Moreover, the standard observer sensitivities transformed to RGB are typically different from the camera spectral sensitivities. Therefore, the colors seen by the camera are different from the standard sRGB colors. Figures 2 and 3 show colors of Gretag-Macbeth ColorChecker chart [5] illuminated with the standard D65 and F12 illuminants and observed by two different cameras: Nokia N900 and Canon EOS 1D Mark III. Sensor spectral sensitivities of these two cameras are shown in Figure 4. Both spectra have been downloaded from RIT database [9].

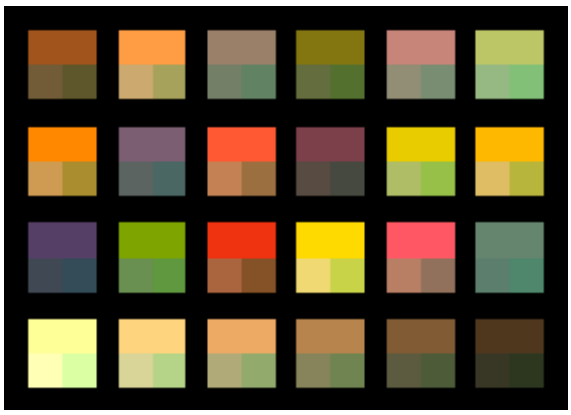

***Figure 3**. Simulated colors of the ColorChecker chart under the standard illuminant F12 seen by two cameras (bottom row at each patch) and reference standard observer simulation based sRGB colors (top row at each patch).*

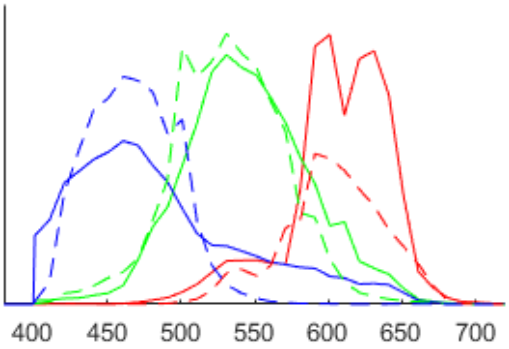


***Figure 4**. Spectral power distribution of sensor spectral sensitivities of Nokia N900 (solid lines) and Canon EOS 1D Mark III (dashed lines) for red, blue and green pixels, over a range of visible spectrum (380 nm – 700 nm).*

Because the camera RGB colors are different from the standard color space colors originating from the same captured data, we need a color transform that maps the camera RGB color coordinates to the standard color coordinates. Otherwise the colors will render incorrectly in a display device calibrated to the standard color space viewing.

$$[R\ G\ B]_{sRGB} = T([R\ G\ B]_{camera}) = T([C_R\ C_G\ C_B]) \qquad (2)$$

Transform $T$ can be either a (3x3 or larger) color correction matrix or a look-up-table (LUT) [14]. With the equation (1) we can calculate the transform using spectral data only ($S_{camera}(\lambda)$, $S_{standard}(\lambda)$, $I(\lambda)$, $R(\lambda)$). Transform $T$ is chosen such that minimizes colorimetric residual errors [4]. From practical point of view, spectra-based color correction provides broader flexibility and easiness of performing computations with different illuminants and large set of reflectances from different test patches or even natural color measurements, as opposed to the chart-based method with real captures of test charts under various calibration illuminants. A result with LUTs optimized for each camera separately and transforming camera RGB of the ColorChecker patches under D65 illuminant to sRGB D65 colors is shown in Figure 5.

The color transform can also include color constancy or chromatic adaptation model [11]. For example, if we want that the transform produces color constant colors as those are seen under D65 illuminant we can set the target for the transform to be D65 standard colors calculated with the equation (2).

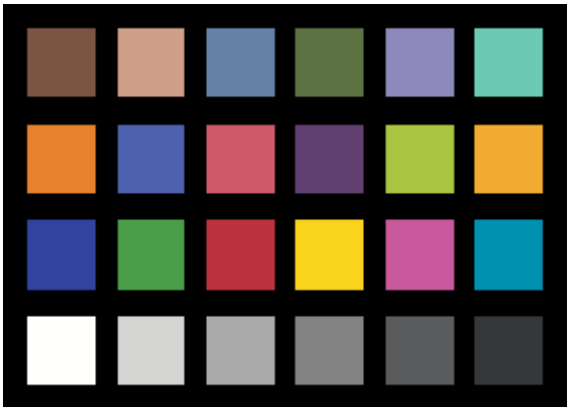

***Figure 5**. Colors of figure 2 (D65) transformed with a LUT optimized for ColorChecker colors from camera RGB under illuminant D65 to sRGB D65. Reference colors at top row of each patch same as in figure 2 (D65).*

Color constancy is achieved within the limits of the accuracy of the chosen transform and metamerism. Without color constancy, the target would be standard colors under the same illuminant. If a chromatic adaptation model is wanted, the target can be modified accordingly or a model applied to the transformed data. Figure 6 shows the result of a LUT transforming F12 camera colors to standard observer F12 colors in sRGB without any chromatic

***Figure 6**. Colors of figure 3 (F12) transformed with a LUT optimized for ColorChecker colors from camera RGB under illuminant F12 to standard observer simulation based sRGB colors. Reference colors at top row of each patch same as in figure 3 (F12).*

adaptation. With full color constancy, the result is looking the same as in the Figure 5.

Due to the fact that camera spectral sensitivities differ at each wavelength, an accurate transform is source illuminant dependent and needs to be calculated individually for each illuminant spectrum. For example, if there is a larger difference in the spectral sensitivities at longer wavelengths the illuminants that have more energy in the longer wavelengths will produce more difference to color patches reflecting the long wavelength than illuminants that have more energy on the shorter wavelengths. Figures 7 and 8 show the result of applying a D65-optimized color transform on colors observed under F12. It is seen that the target colors are not reached, either with (Figure 8) or without (Figure 7) the color constancy target. It is also seen that there is difference between the two example cameras, in case of illuminant specific transform the colors captured with different cameras match (see carefully e.g. patches 2, 4, 9, 14 and 15). This is an important aspect of a 360º capture with multiple cameras. The reconstruction of the 360º scene from multiple captures from separate cameras becomes easier when the colors are accurate and matching well between individual cameras.

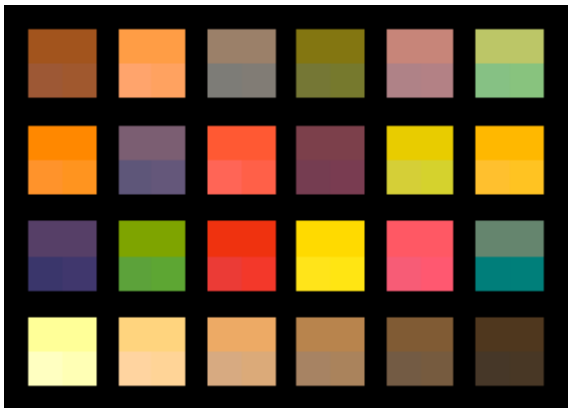

***Figure 7**. Colors of figure 3 (F12) transformed with a LUT optimized for ColorChecker colors from camera RGB under illuminant D65 to sRGB D65. Reference colors at top row of each patch same as in figure 3 (F12).*

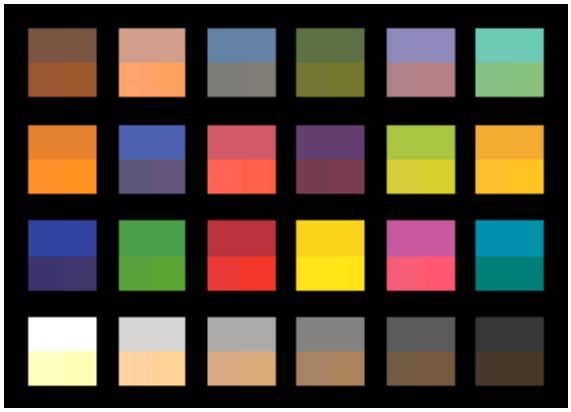

***Figure 8**. Colors of figure 3 (F12) transformed with a LUT optimized for ColorChecker colors from camera RGB under illuminant D65 to sRGB D65. Reference colors at top row of each patch same as in figure 2 (D65).*

## Results

In practical applications color transforms need to be optimized for discrete illuminants. An often used set of illuminants consists of the CIE standardized illuminants [6]. However, as camera measurements are executed with real world light sources, there can be a discrepancy between these two. When a F12 standard spectra [12] was compared to e.g. an Image Engineering LightStudio [7] F12 illuminant, a clear difference was noted. Figure 9 shows a divergence especially in blue wavelengths as well as in the amplitude of the peaks.

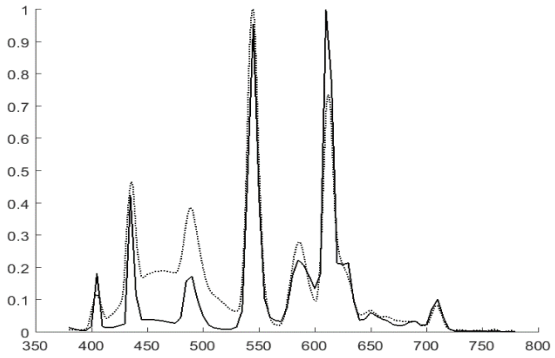


***Figure 9**. Spectrums of CIE F12 standard illuminant (solid line) and LightStudio F12 illuminant (dotted line).*

If a color correction of a camera system is done using the standard spectra, this difference may also cause an unwanted tint and color errors to images. A clear evidence for this phenomenon was found when a footage was captured using Nokia OZO Virtual Reality Camera [8] from a LightStudio interior using the F12 illuminant. When colors were inspected visually using X-Rite ColorChecker chart [5] and corresponding color differences were calculated using CIEDE2000 ΔC-00 chrominance error values, especially light skin tone (color patch number two) had a pinkish tint. The same phenomenon was visible in the LightStudio image containing ladies' faces (Figure 12).

A positive improvement was noted when the color transform was re-optimized using a custom illuminant based on a measured spectrum of the LightStudio F12 illuminant. An average ΔC-00 was decreased from 4.6 to 2.6. Most of the colors which were outside

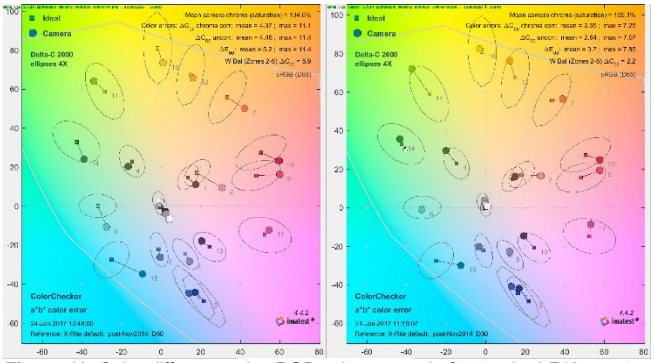

***Figure 10**. Color differences in sRGB color space. Left: standard F12 spectra, right: measured spectra.*

4xMacAdams ellipses [13] were now located inside. Even if chrominance error of some color patches increased, the corresponding errors were still inside MacAdams ellipses or on the ellipse border line. In general, the overall color change was clearly positive. Figure 10 shows the improvement of all color patches.

Visually, the improvement was clear. Especially a light skin tone, which is one of the memory colors and thus very vulnerable to color tint, was changed from pinkish tint to a more correct one. Figures 11 and 12 show the difference in the second color patch and skin tones of ladies correspondingly. Specific ΔC-00 values of all patches can be found from Table 1.

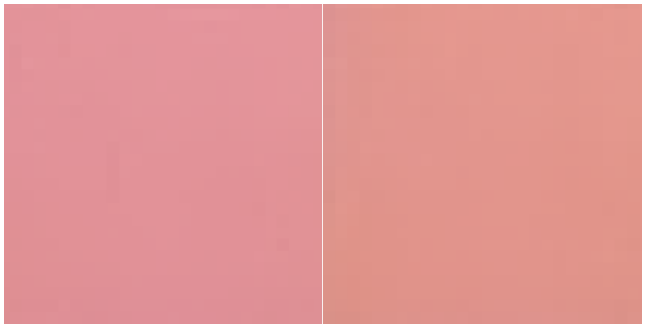

***Figure 11**. Color difference in the light skin tone patch. Left: standard F12 spectra, right: measured spectra.*

***Figure 12**. Color difference on the real skin. Left: standard F12 spectra, right: measured spectra.*

**Table 1. CIE ΔC-00 values from X-Rite ColorChecker**

| Patch # | Standard spectra | Custom spectra |
|---|---|---|
| 1 | 5.0 | 1.2 |
| 2 | 10.4 | 5.9 |
| 3 | 1.6 | 2.1 |
| 4 | 2.4 | 3.6 |
| 5 | 1.9 | 1.1 |
| 6 | 8.0 | 0.8 |
| 7 | 6.8 | 2.8 |
| 8 | 1.6 | 1.2 |
| 9 | 3.6 | 3.0 |
| 10 | 2.1 | 3.7 |
| 11 | 2.1 | 3.8 |
| 12 | 1.1 | 3.3 |
| 13 | 1.7 | 2.1 |
| 14 | 3.7 | 1.0 |
| 15 | 4.7 | 3.5 |
| 16 | 2.5 | 0.7 |
| 17 | 1.3 | 2.8 |
| 18 | 9.7 | 7.1 |
| 19 | 11.6 | 3.7 |
| 20 | 8.7 | 1.4 |
| 21 | 6.1 | 3.5 |
| 22 | 4.8 | 2.2 |
| 23 | 5.0 | 1.6 |
| 24 | 4.0 | 1.5 |

In another experiment, we have measured impact of a spatially mixed illuminant spectra on the colorimetric error. Figure 13 presents the experiment setup: 3D 360º camera with an overlap between each of its neighbouring sensors. Several instances of the same test targets (X-Rite ColorCheckers and LightStudio's image containing ladies' faces) have been placed in three areas: 1) illuminated by D65 light source and seen by left sensor only, 2) illuminated by halogen A light source and visible only to the right sensor, 3) illuminated by mixed D65 and A light, visible by both sensors. The last case is the most important from the 360º camera point of view, as it is perceived as a "seam" area during the content stitching.

If we were to perform the colour mapping of the seam area while using either D65 or A standard illuminants as a source to the equation (1), we would not only obtain large colorimetric errors, but also produce unpleasantly looking stitched image. This can be clearly seen at the Figure 13 on the left. Measuring the spatially varying custom illuminant spectrum and using it as a source for the colour transform optimization, the results are unsurprisingly superior to the standard illuminant case. Color differences were calculated using CIEDE2000 ΔC-00 chrominance error and are presented in the Table 2.

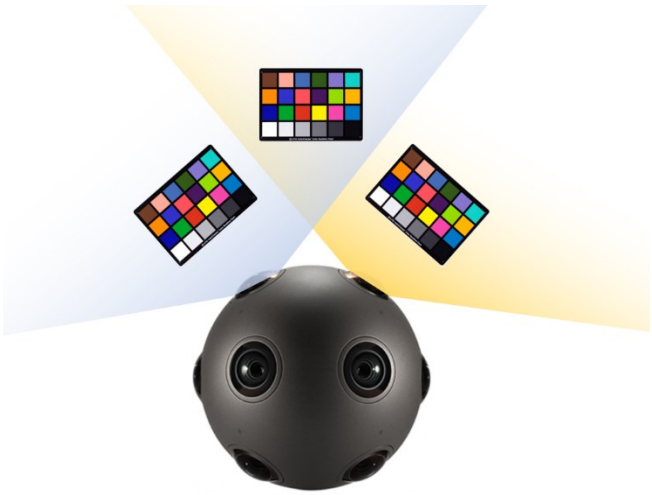

***Figure 13.*** *3D 360º camera observing scene under different illuminants. Two sensors on the top observe three instances of the X-Rite ColorChecker under different illuminations (from left to right): D65 (blue glow), mixed D65 + A, and halogen (yellow glow).*

***Figure 14.*** *On the left: seam area processed with two different illuminants: D65 (left) and A (right). On the right: the same image processed with measured custom illuminant comprising D65 and A illuminant.*

**Table 2. CIE ΔC-00 values from X-Rite ColorChecker in case of exposure to spatially mixed illuminant and processed with different source illuminants: D65, A and custom spectrum.**

| Patch # | D65 | A | Custom |
|---|---|---|---|
| 1 | 6.9 | 6.1 | 2.0 |
| 2 | 10.5 | 8.8 | 2.4 |
| 3 | 14.4 | 2.8 | 1.8 |
| 4 | 8.5 | 5.0 | 1.4 |
| 5 | 16.8 | 6.1 | 1.7 |
| 6 | 13.6 | 9.3 | 1.0 |
| 7 | 6.3 | 3.0 | 1.2 |
| 8 | 11.0 | 1.8 | 1.6 |
| 9 | 10.0 | 4.2 | 1.3 |
| 10 | 12.7 | 4.9 | 3.8 |
| 11 | 8.4 | 4.2 | 2.3 |
| 12 | 8.1 | 4.0 | 1.2 |
| 13 | 8.6 | 2.0 | 2.7 |
| 14 | 7.3 | 2.9 | 1.7 |
| 15 | 6.2 | 4.4 | 1.6 |
| 16 | 9.4 | 4.6 | 1.4 |
| 17 | 14.8 | 3.3 | 3.0 |
| 18 | 13.0 | 9.4 | 5.7 |
| 19 | 16.8 | 13.9 | 1.3 |
| 20 | 19.8 | 9.8 | 2.4 |
| 21 | 18.5 | 7.4 | 3.8 |
| 22 | 15.5 | 6.1 | 4.2 |
| 23 | 13.4 | 4.5 | 3.0 |
| 24 | 11.3 | 3.1 | 3.4 |

## Conclusions

We have demonstrated how even small changes in either camera spectral sensitivities or illuminant spectra can cause clearly visible differences in the produced colors. We have explored this problem from the point-of-view of a 3D 360º camera, which to the best of our knowledge, has not been done before.

Color constancy at the camera center is an enabler for more sophisticated spectral color correction. As future work, we have set for ourselves an exploration of a problem of a spatially varying illumination and its influence on color accuracy in a stereo-panoramic use case. It will be interesting to see how this information can be utilized for overall image stitching improvements when e.g. combined with spatial map of camera spectral sensor sensitivities.

## References


[1] A. Gijsenij, T. Gevers, and J. van de Weijer. “Computational color constancy: Survey and experiments”. IEEE Transactions on Image Processing, 20(9), 2011.

[2] C. Mauer. “Measurement of the spectral response of digital cameras”. VDM Verlag Dr. Miller, 2010

[3] R. Nguyen, D.K. Prasad, M.S. Brown. "Raw-to-raw: Mapping between image sensor color responses". CVPR, 2014

[4] F. Martinez-Verdu, J. Pujol, and P. Capilla. “Characterization of a digital camera as an absolute tristimulus colorimeter”. Journal of Imaging Science and Technology, 47(4):279–295, 2003.

[5] X-Rite Color Checker chart, Homepage, Cited 16th of February 2017. http://xritephoto.com/colorchecker-classic.

[6] International Commission on Illumination, CIE 15.3, Colorimetry 3rd Edition, 2004.

[7] Image Engineering LightStudio, Homepage, Cited 16th of February 2017. http:// https://www.image-engineering.de/products/equipment/illumination-devices/382-modular-lightstudio.

[8] Nokia OZO Virtual Reality Camera, Homepage, Cited 24th of February 2017. https://ozo.nokia.com.

[9] Dengyu Liu, Space of Spectral Sensitivity Functions for Digital Color Cameras, Project webpage, Cited 24th of February 2017, http://www.cis.rit.edu/~dxl5849/projects/camspec/database.txt

[10] J. Nakamura. "Image Sensors and Signal Processing for Digital Still Cameras". CRC Press, 2006.

[11] Mark D. Fairchild. “Color Appearance Models”, 3rd Ed. Wiley-IS&T, Chichester, UK, 2013.

[12] Rochester Institute of Technology, Homepage, Cited 13th of February 2017. http:// http://www.rit.edu/cos/colorscience/rc_useful_data.php.

[13] G. Wyszecki, W.S. Stiles. „Color Science”, 2nd edition, A Wiley-Interscience Publication, New York, 2000.

[14] P. Hung. “Colorimetric calibration in electronic imaging devices using a look-up tables model and interpolations”. Journal of Electronic Imaging, vol. 2, no. 1, pp. 53-61, 1993.